Proteus syndrome - Manuscript Submission V5.6

Manuscript title:

Misaligned foveal morphology and sector retinal dysfunction in AKT1-mosaic Proteus Syndrome.

Authors:

First author:

Oliver R. Marmoy[1,2] (*ORCID ID: 0000-0003-2022-3369)*

Second author:

Veronica A. Kinsler [3,4] (*ORCID ID: 0000-0001-6256-327X)*

Third author:

Robert H. Henderson [1,4] (*ORCID ID: 0000-0002-5250-6404)*

Fourth author:

Sian E. Handley [1,4] (*ORCID ID: 0000-0002-7612-3889)*

Fifth author:

Will Moore [1] (*ORCID ID: N/A)*

Sixth author:

Dorothy A. Thompson [1,4] (*ORCID ID: 0000-0001-5491-3911)*

Author affiliations:

1 – Clinical and Academic Department of Ophthalmology, Great Ormond Street Hospital for Children, London, UK

2 – Manchester Metropolitan University, Manchester, UK

3 – Paediatric Dermatology, Great Ormond Street Hospital for Children, London, UK

4 – UCL-GOSH Institute of Child Health, University College London, London, UK

Corresponding author:

Oliver R. Marmoy (O.Marmoy@nhs.net). Present address is as described above as number 1 and is the main affiliation address.

Author declaration:

All authors approve to the final version of the manuscript and are collectively accountable for all aspects of the work. All persons designated as authors qualify for authorship.

Acknowledgements:

None to declare.

Funding:

No funding received.

Competing interests:

No conflict of interest to disclose.

Abstract:

Proteus syndrome arises as a result of a post-zygotic mosaic activating mutation in the *AKT1* oncogene, resulting in disproportionate overgrowth of affected tissues. A number of ocular complications have also been reported. We present a unique finding in a patient with Proteus syndrome, fulfilling the clinical criteria with molecular confirmation (3)(15), who was found to have misaligned foveal architecture and additional segmental retinal dysfunction in her right eye. Pattern electroretinography and multi-focal ERG findings demonstrate retinal dysfunction, which was correlated with structural alterations identified with ultrawide-field imaging and optical coherence tomography of the maculae. We propose this patient has an asymmetric development of her fovea as the result of *AKT1* mutation, either through disruption in the *AKT1* pathway or disproportionate inner retinal growth.

Introduction

Proteus syndrome (PS) is a rare condition which causes overgrowth of many tissues with a wide phenotypic variation [1]. These findings are uniquely the result of a recurrent post-zygotic mosaic variant in the *AKT1* oncogene [2]. Clear clinical criteria have been defined, which differentiate this condition from other segmental overgrowth disorders [3]. Fulfilment of the criteria require a mosaic distribution of lesions, spontaneous occurrence and progressive course. Although genetic confirmation of AKT1 mosaicism may contribute to the clinical diagnosis of PS, AKT1 mosaicism alone is not pathognomonic for a diagnosis of PS [4].

There have been a number of reports detailing the ophthalmic complications associated with PS with a wide phenotypic variation including strabismus, nystagmus, retinal pigmentary abnormalities, cataract, optic nerve anomalies and hamartomas [5, 6, 7] . Many of the reported case series of ophthalmic involvement in PS pre-date the introduction of strict clinical criteria and genetic basis, which explains the wide ophthalmic phenotype. The missense change in AKT1 (c.49G>A, p.(Glu17Lys)) was identified with unique features suggesting PS is a distinct clinical and genetic entity compared to other segmental overgrowth syndromes [2,8]. This more recent classification suggests some earlier literature may report ophthalmic complications associated with separate segmental overgrowth syndromes that are different from our current understanding of Proteus syndrome. Turner et al. reassessed the PS literature and demonstrated that only 47.3% of published cases met the diagnostic criteria for PS [1]. Despite this, subsequent reports meeting the new diagnostic criteria with genetic basis still show a broad ocular polymorphism, but empirical ophthalmic investigation in PS is still lacking [5, 7, 9-12]..

The phenotypic heterogeneity in Proteus syndrome warrants an ophthalmic examination in all patients with this rare condition. We describe a 12-year-old female patient diagnosed with Proteus syndrome who attended for ophthalmic review with no visual complaints. Unexpectedly we found a highly unusual ocular phenotype of unilateral foveal misalignment and sector retinal dysfunction, which to the best of our knowledge has not been reported in a patient with *AKT1* mosaicism.

Case report

We describe a twelve-year-old female with a mild phenotype of *AKT1* mosaicism. Her first sign was a keratinocytic epidermal naevus on her right cheek identified when she was 5yrs old. This epidermal

naevus slowly progressed to fullness over her periauricular and mandibular areas resulting in hemihypertrophy. Magnetic resonance imaging (MRI) age six years demonstrated asymmetry of facial tissues, with an additional focal osteoma in the right external auditory canal associated with a maximal conductive hearing loss in the right ear. Further examination age seven revealed hemihypertrophy of her tongue with misaligned teeth and asymmetric pigmentation differences within the right side of the oral cavity. At age eight years MRI revealed asymmetric skull overgrowth of the right forehead. Genetic studies demonstrated a somatic activating mutation (c.49G>A, p.Glu17Lys) in the oncogene *AKT1* and she fulfilled the strict diagnostic criteria for PS [3]. This patient's clinical and genetic features have been described previously [13].

The genetic diagnosis and right skull overgrowth prompted an ophthalmic review. Initial examination recorded subnormal right eye (RE) visual acuity of LogMAR 1.300 ,but normal left eye (LE) acuity -0.060; Ishihara colour vision was subnormal RE, 6/11 plates and normal LE, 11/11 plates. Cycloplegic refraction was more myopic in the RE, with RE -1.25/-0.25x90 and LE +0.25/ 0.25x100. The anterior segment, inter-ocular pressure and optic nerve appearance were within normal limits. There was no relative afferent pupil defect and ocular movements were full, with no evidence of strabismus to the Hirschberg test. The RE fundus appeared to have paramacular and peripheral pigmentary changes and the LE had a normal fundus appearance).

The patient was referred for visual electrophysiology testing and ocular imaging. Ultrawide-field fundus imaging (OPTOS®, Dunfermline) to red-green colour and fundus autofluorescence were unremarkable in the LE (Figure 1c &1d), but the RE demonstrated diffuse, mottled pigmentary changes in the periphery, with increased hyper- fundus auto fluorescence (FAF) at the macula, extending horizontally and peripherally towards the inferior-temporal retina (Figure 1a & 1b). Optomap imaging, whilst not true-colour, utilises red and green lasers to construct a colour ultra-wide field image which utilises the characteristics that red lasers have deeper penetration to scan

from the RPE to choroid, whereas green laser from the sensory retina to RPE superficial layers. Axial Optical Coherence Tomography (OCT) (Spectralis ,Heidelberg Engineering Inc.) was performed performing axial single scans and through volumetric scans across the maculae. The macular layers were segmented and the Outer Nuclear Layer (ONL) and Retinal Ganglion Cell Layer (RGCL) thicknesses observed as a function of thickness at each macular (Figure g-j). These showed an atypical foveal architecture in the RE, where the characteristic distal foveal thickening of the outer nuclear layer was markedly misaligned and displaced temporally with respect to the foveal pit alongside sectoral atrophy of the outer retinal layers seen (Figure 1e, 1g, 1h), unlike the left macular which was normally formed (Figure 1f, 1i, 1j).

Figure 1 around here (legend in appendices)

Pattern reversal VEPs (prVEPs) were obtained from a transoccipital electrode array referred to Fz with a 250ms epoch time-locked to a large (30°) field high contrast pattern stimulus reversing at 3 rev/sec to large (50') and small (12.5') check widths comparable to ISCEV standards [14]. The prVEPs from the RE produced a highly atypical broad bifid waveform comprising early and late positive peaks which were time-locked to the stimulus, rather than spurious as would be expected with noise/background electroencephalogram activity. Those from the LE were within normal reference limits (92-115ms) (Figure 2). Pattern electroretinograms (PERGs) were recorded using DTL fibre electrodes referred to an outer canthus electrode produced to a range of check widths presented binocularly in a large (30°) and small (14°) field with high contrast at a 3rev/sec rate in line with ISCEV standards [15]. The PERG from the 30 degree field showed a subtle inter-ocular difference of P50 reduction and delay which appeared more evident to higher spatial frequencies, with the 14 degree field PERG also demonstrating P50 amplitude reduction and delay in the RE relative to the LE (Figure 2). Multi-focal ERGs (mfERG) were recorded to a 61 hexagon stimulus with DTL fibre electrodes referred to an outer canthus reference binocularly to ISCEV standards [16] after pupil dilation and refractive correction demonstrated typical macular response topography in the LE,

however the RE mfERG showed a reduced foveal peak with broad, small responses from the temporal macular area concordant with the anomalous imaging findings (Figure 2). MfERGs and PERGs were also recorded monocularly after binocular testing to exclude potential for eccentric fixation, though this is unlikely as the patient had central fixation during OCT testing (supplementary figure 1). All electrophysiological data was recorded using the same equipment (Diagnosys LLC, Cambridge, UK). Previous MRIs were re-examined and very subtle globe asymmetry was detected with subtle nasal flattening and bulging of the temporal globe of the RE (Figure 1).

Figure 2 around here (legend in appendices)

Discussion

Proteus syndrome is consequent upon a somatic activating mutation of *AKT1*, encoding AKT1 kinase, an enzyme responsible for cell proliferation and apoptosis [2]. This case has uniquely demonstrated that the reported symptomology of Proteus syndrome, largely comprising asymmetric tissue overgrowth, can manifest within the retina. This patient's ocular phenotype of an unusual misaligned foveal architecture and segmental retinal dysfunction in association with with *AKT1* mosaicism has not been previously reported to our knowledge.

AKT1 is a downstream effector of phosphoinositide 3-kinase (P13K), with its activation shown to improve cell survival. *AKT1* is one of three *AKT* isoforms. Although *AKT2* and *AKT3* are similar biologically, their mode of activation and function are distinct [17]. Activation of *AKT1* has been demonstrated to be an important moderator of metabolism, apoptosis and transcription processing in a variety of retinal genes [18,19]. Two protein phosphatases, PHLPP and PHLPPL, that control downstream *AKT* signalling are expressed in the retina and play an essential role in retinal neuroprotection [20,21]. An impairment of the P13K/AKT pathway can disrupt these phosphatases causing unregulated photoreceptor metabolism and apoptosis [22]. In our patient, we observed

distal photoreceptor atrophy of the temporal macula region extending into the periphery, which may be concordant with disturbed PHLPP-PHLPPL phosphatase function resulting in photoreceptor death. It is interesting in our patient that the inner retinal structure remained mostly undisturbed, suggesting that *AKT* kinase isoforms play a role in photoreceptor neuroprotection and not bipolar or horizontal cell neuroprotection. This view would be supported by studies examining light-induced cell death properties of *Akt1* in mice, where *Akt1* was found to bind to rod-photoreceptor outer-segments [20]. It has been proposed in *Akt1* knockout mice that *Akt1* deletion has little effect on photoreceptor cell death, rather *Akt2* disruption is more accountable for light-induced apoptosis [21]. The AKT2 isoform is a key mediator of insulin action, as such its dysfunction results in mild overgrowth, but also severe insulin dependent hypoglycaemia and progressive obesity. These features were not evident in our patient [23,24]. It seems that light exposure would play a minimal role in the progression of retinal dysfunction in isolated *AKT1* mutations.

The structural foveal misalignment found in our patient is highly unusual. The potential mechanism behind this is complex and likely involves an interplay of factors. It is known that during foveal development, cone photoreceptors exhibit tight 'packing' whilst elongating through concentric migration toward the fovea [25,26]. Although the later formation and specialisation of the inner retina and depends upon centrifugal migration of cells away from the fovea, the exact mechanisms of foveal pit generation and its relationship with the cone-packing migration remains uncertain [27]. Given that the development of the fovea occurs concentrically, it is highly unusual that this patient exhibited horizontal distortion of her foveal pit in relation to the outer plexiform thickening (OPL). Comparison with this patient's normal fellow left eye (LE) demonstrated that the outer plexiform thickening was symmetrical for each eye, at the fovea centralis, whereas it appears that the inner retinal layers forming the foveal pit were displaced laterally in the right (RE), but with symmetrical morphology. It may be, therefore, that there is disjointed communication between the centripetal elongation and packing of cone photoreceptors into the fovea versus the centrifugal movement of

inner retinal neurons from the fovea. The mechanism behind this change is uncertain and it is possible that this structural displacement was acquired later in the patient's development and after normal foveal development.

The first theory would be that the disjointed signalling might be due to the mutation affecting the activation of the PI3K-AKT pathway during a critical period of retinal specialisation and foveal development. A second theory would be that this change is secondary to the AKT1-P13K disruption resulting in the sectoral retinal atrophy [2]). It has been demonstrated in-vivo that inner-retinal layers migrate before outer retinal layers during foveal development, with full maturation lasting until at least twelve years of age [28]. However, previous studies have described that inner retinal centrifugal migration is complete between 6-40 weeks post-natally [29]. In the developing retina, mosaicly formed neurons move tangentially to accommodate new cells and preserve regular cell spacing [29,30]. *AKT1* mutations can manifest at any age of development [2]. Therefore, a localised dystrophic process in the retina during this period of critical specialisation may have resulted in loss of cellular homogeneity disrupting the mechanical retinal cell assembly and/or signalling, causing a misaligned foveal architecture.

A third theory may be asymmetric mechanical distortion of the inner retina. It has previously been proposed that mechanical stretching of the retina through growth controls this migration of inner retinal layers [31], which was confirmed in-vivo [28]. It is possible that the patient has subtle orbital asymmetry, resultant or coexisting with her right forehead overgrowth, which may be related to the small myopic astigmatism. A potential orbital asymmetry may affected the migration of inner retinal neurons through asymmetric retinal stretching, where the foveal dip has been laterally shifted and affected more than outer retinal layers. The differences between the migration trajectories and time for complete migration would be compromised and could account for this disproportionate and

misaligned fovea. Conversely, it is known that disruption in the PI3K-AKT pathway may contribute to myopia progression, which in its mosaic form may have only been expressed in the temporal globe in our patient and therefore may reflect a change that occurred after foveal differentiation [32,33].

Multifocal electroretinography shows reduced retinal sensitivity over the temporal dystrophic outer layers of the RE. Perhaps most interestingly, the mfERG response from the 'foveal' hexagon was smaller relative to hexagons horizontally adjacent. This finding was verified by testing monocularly following binocular testing, with central fixation confirmed from the en-face OCT view. Within mfERG, responses, an initial negative component (N1) originating from off-bipolar and photoreceptor cells is shortly after followed by a positive response (P2) from on- and off-bipolar cells in the healthy retina [34]. Although contributions from photoreceptor cells to the N1 are higher in the central foveolar in our case, there is an attenuated foveal peak which indicates low foveal cone photoreceptor contribution. In contrast, P1 bipolar cell derived components appear preserved over the area of skewed outer segment bunching, where we may expect the high density of cone photoreceptors. This suggests that the functional integrity of the photoreceptor-bipolar interface in this distorted fovea is preserved sufficiently enough to allow signal transduction.

This further supports the mechanical distortion theory. The PERGs produced by smaller check widths emphasised the inter-ocular difference, but due to the spatial summation the PERG slightly underestimates the extent of macula dysfunction and the mfERG provided more valuable functional information of localised retinal topography. Nevertheless, the findings highlight the benefit of both large and smaller ISCEV standard field size PERGs to provide some information of the extent of macula dysfunction.

Conclusion

We demonstrate a unique case of foveal misalignment and sector retinal dysfunction in a patient with *AKT1* mosaicism who fulfils the criteria for Proteus syndrome. Our findings expand the clinical ocular phenotype of this rare genetic disease and present a new and highly unusual retinal dysmorphism which to our knowledge, has not been reported previously. To account for these unusual findings we have proposed disruption of the AKT1-P13K pathway and/or inner-outer layer growth miscommunication as potential mechanisms, alongside a theory of mechanical distortion due to myopic changes or triggers in globe shape. As our patient had no complaints of visual symptoms prior to our investigations, despite an large inter-ocular acuity difference, it seems prudent for all patients with Proteus syndrome, who often have asymmetric tissue involvement, to have ophthalmological assessment to exclude underlying ophthalmic disease. Imaging and visual electrophysiology were important in this case to delineate the structural and functional consequences of *AKT1* mosaicism in the eye.

Patient consent:

Institutional research approvals were given for this case-note review (reference: 19SS12); patient consent was waived by the IRB for use of these anonymised data.

References

1- Turner J T, Cohen M M and Biesecker L G. (2004). *Reassessment of the Proteus Syndrome Literature: Application of Diagnostic Criteria to Published Cases.* American Journal of Medical Genetics, Vol. 130: 111-122. DOI: 10.1002/ajmg.a.30327.

2- Lindhurst M J, Sapp J C, Teer J K, Johnston J J, Finn E M, Peters K, et al. (2011). *A Mosaic Activating Mutation in AKT1 Associated with the Proteus Syndrome.* New England Journal of Medicine, Vol. 365(7): 611-619. DOI: 10.1056/NEJMoa1104017.

3- Biesecker L G, Happle R and Mulliken J B, Weksberg R, Graham J M Jr, Viljoen D L and Cohen M M Jr. (1999). *Proteus syndrome: diagnostic criteria, differential diagnosis and patient evaulation.* American Journal of Medical Genetics, Vol. 84(5): 389-395. DOI: 10.1002/(sici)1096-8628(19990611)84:5<389::aid-ajmg1>3.0.co;2-o

4- Wee J S, Mortimer P S, Lindhurst M J, Chong H, Biesecker L G and Holden C A. (2014). *A limited form of proteus syndrome with bilateral plantar cerebriform collagenomas and varicose veins secondary to a mosaic AKT1 mutation.* JAMA Dermatology, Vol. 150(9): 990-993. DOI: 10.1001/jamadermatol.2013.10368.

5- De Becker I, Gajda D J, Gilbert-Barness E and Cohen, M M Jr. (2000). *Ocular Manifestations in Proteus Syndrome.* American Journal of Medical Genetics, Vol. 92(5): 350-352. DOI: https://doi.org/10.1002/1096-8628(20000619)92:5<350::AID-AJMG11>3.0.CO;2-O.

6- Burke J P, Bowell R and O'Doherty N. (1988). *Proteus Syndrome: Ocular Complications.* Journal of Pediatric Ophthalmology and Strabismus, Vol. 25(2): 99-102.

7- Trivedi D, Lee S Y, Brundler M A and Parulekar M V. (2013). *Fibrous tumour of the superior oblique tendon in Proteus syndrome.* Journal of Americal Association for Pediatric Ophthalmology and Strabismus, Vol. 17(4): 420-422. DOI: 10.1016/j.jaapos.2013.03.019.

8- Cohen, M M Jr. (2014). *Proteus syndrome review: molecular, clinical, and pathologic features.* Clinical Genetics, Vol. 85(2): 111-119. DOI: 10.1111/cge.12266.

9- Mirshahi A, Mohammadi, S-M and MirMohammadSadeghi, A. (2009). *Proteus Syndrome: A case Report of General and Ophthalmic Findings.* Iranian Society of Ophthalmology, Vol. 21(1): 65-69.

10- Sheard R M, Pope M F and Snead, M P. (2002). A *Novel Ophthalmic Presentation of the Proteus Syndrome.* Ophthalmology, Vol. 109(6): 1192-1195. DOI: 10.1016/S0161-6420(02)01056-4.

11- Russell-Hermanns D S and Newman D K. (2017). *Rhegmatogenous retinal detachment: A rare ocular manifestation of Proteus Syndrome.* Retinal Cases & Brief Reports, Vol. 11(3):283-285. DOI: 10.1097/ICB.0000000000000347.

12- Bouzas E A, Krasnewich D, Koutrousmanidis M, Papadimitriou A, Marini J C and Kaiser-Kupfer M I. (1993). *Ophthalmologic Examination in the Diagnosis of Proteus Syndrome.* Ophthalmology, Vol. 100(3): 334-338. DOI: 10.1016/s0161-6420(93)31645-3

13- Polubothu S, Al-Olabi L, Wilson L, Chong W K and Kinsler V A. (2016). *Extending the spectrum of AKT1 mosaicism: not just the Proteus syndrome.* The British Journal of Dermatology, Vol. 175(3): 612-614. DOI: 10.1111/bjd.14478.

14- Odom J V, Bach M, Brigell M, Holder G E, McCulloch D L, Mizota A and Tormene A P. (2016). *ISCEV standard for clinical visual evoked potentials: (2016 update).* Documenta Ophthalmologica, Vol. 133(1): 1-9. DOI: 10.1007/s10633-016-9553-y.

15- Bach M, Brigell M G, Hawlina M, Holder G E, Johnson M A, McCulloch D L Meigen T and Viswanathan, S. (2013). *ISCEV standard for clinical pattern electroretinography (PERG): 2012 update.* Documenta Ophthalmologica, Vol. 126(1): 1-7. DOI: 10.1007/s10633-012-9353-y.

16- Hood D C, Bach M, Brigell M, Keating D, Kondo M, Lyons J S, Marmor M F, McCulloch D L and Palmowski-Wolfe A M. (2012). *ISCEV standard for clinical multifocal electroretinography*

(mfERG) (2011 edition). Documenta Ophthalmologica, Vol. 124(1): 1-13. DOI: 10.1007/s10633-011-9296-8.

17- Santi S A, Douglas A C and Lee H. (2010). *The Akt isoforms, their unique functions and potential as anticancer therapeutic targets.* Biomolecular Concepts, Vol. 1(5-6): 389-401. DOI: 10.1515/bmc.2010.035.

18- New D C, Wu K, Kwok A W and Wong Y H. (2007). G *protein-coupled receptor-induced Akt activity in ceulluar proliferation and apoptosis.*, FEBS Journal, Vol. 274(23): 6025-6036.

19- Parcellier A, Tintignac L A, Zhuravleva E and Hemmings B A. (2008). *PKB and the mitrochondria: AKTing on apoptosis*. Cell Signal, Vol. 20(1): 21-30.

20- Li G, Rajala A, Wiechmann A F, Anderson R E and Rajala R V. (2008). *Activation and membrane binding of retinal protein kinase Balpha/Akt1 is regulated through light-dependent generation of phosphoinositides.* Journal of Neurochemistry, Vol. 107(5): 1382-1397. DOI: 10.1111/j.1471-4159.2008.05707.x.

21- Li G, Anderson R E, Tomita H, Adler R, Liu X, Zack D J and Rajala R V. (2007). *Nonredundant role of Akt2 for neuroprotection of rod photoreceptor cells from light-induced cell death.* Journal of Neuroscience, Vol. 27(1): 203-211. DOI: 10.1523/JNEUROSCI.0445-06.2007.

22- Mackey A, Sanvicens N, Groeger G, Doonan F, Wallace D and Cotter T G. (2008). *Redox survival signalling in retina-derived 661W cells.* Cell Death and Differentiation, Vol. 15(8): 1291-1303. DOI: 10.1038/cdd.2008.43.

23- Leiter S M, Parker V E R, Welters A, Knox R, Rocha N, Clark G, Payne F, Lotta L, Harris J, et al. (2017). *Hypoinsulinaemic, hypoketotic hypoglycaemia due to mosaic genetic activation of PI3-Kinase.* European Journal of Endocrinology, Vol. 177(2): 175-186. DOI: 10.1530/EJE-17-0132.

24- Hussain K, Bodamer O A F, Cameron F J, Camacho-Hubner C, Soos M A, Jones J, Krywawych S, O'Rahilly S and Aynsley-Green A. (2004). *Hypoketotic hypofattyacidaemic hypoinsulinaemic hypoglycaemia in a child with hemihypertrophy? A new syndrome.* Hormone Research, Vol. 61: 222-227. DOI: 10.1159/000076553.

25- Yuodelis C and Hendrickson A. (1986). *A qualitative and quantitative analysis of the human fovea during development.* Vision Research, Vol. 26(6): 847-855. DOI: 10.1016/0042-6989(86)90143-4.

26- Diaz-Araya C and Provis J M. (1992). *Evidence of photoreceptor migration during early foveal development: a quantitative analysis of human fetal retinae.* Visual Neuroscience, Vol. 8(6): 505-514. DOI: 10.1017/s0952523800005605.

27- Privis J M, Penfold P L, Cornish E E, Sandercoe T M and Madigan M C. (2005). *Anatomy and development of the macular: specialisation and the volnerability to macular degeneration.* Clinical and Experimetnal Optometry, Vol. 88(5): 269-281. DOI: 10.1111/j.1444-0938.2005.tb06711.x.

28- Lee H, Purohit R, Patel A, Papageorgiou E, Sheth V, Maconachie G, Pilat A, McLean R J and Gottlob I. (2015). *In Vivo Foveal Develpment Using Optical Coherence Tomography.* Investigative Ophthalmology and Vision Science, Vol. 56(8): 4527-4545. DOI: 10.1167/iovs.15-16542.

29- Dubis A M, Costakos D M, and Subramaniam C D, Godara P, Wirostko W J, Carroll J and Provis J M. (2012). *Evaluation of normal human foveal development using optical coherence tomography and histologic examination.* Archives of Ophthalmology, Vol. 130(10): 1291-1300. DOI: 10.1001/archophthalmol.2012.2270.

30- Galli-Resta, L. (2002). *Putting neurons in the right places: local interactions in the genesis of retinal architecture.* Trends in Neurosciences, Vol. 25(12): 638-643. DOI: 10.1016/s0166-2236(02)02279-8.

31- Springer A D and Hendrickson A E. (2005). *Development of the primate area of high acuity 3: temporal relationships between pit formation, retinal elongation and cone packing.* Visual Neuroscience, Vol. 22(2): 171-185. DOI: 10.1017/S095252380522206X.

32- Lin H J, Wei C C, Chang C Y, Chen T H, Hsu Y A, Hsieh Y C, Chen H J and Wan L. (2016). *Role of Chronic Inflammation in Myopia Progression: Clinical Evidence and Experimental Validation.*: EBioMedicine, Vol. 10: 269-281. DOI: 10.1016/j.ebiom.2016.07.021.

33- Chen M, Qian Y, Dai J and Chu R. (2014). *The Sonic Hedgehog Signaling Pathway Induces Myopic Development by Activating Matrix Metalloproteinase (MMP)-2 in Guinea Pigs.* PLoS One, Vol. 9(5): e96952. DOI: 10.1371/journal.pone.0096952.

34- Hood D C, Frishman L J, Saszik S and Viswanathan S. (2002). *Retinal origins of the primate multifocal ERG: implications for the human response.* Investigiative Ophthalmology and VIsion Science, Vol. 43(5): 1673-1685.

Figure legends

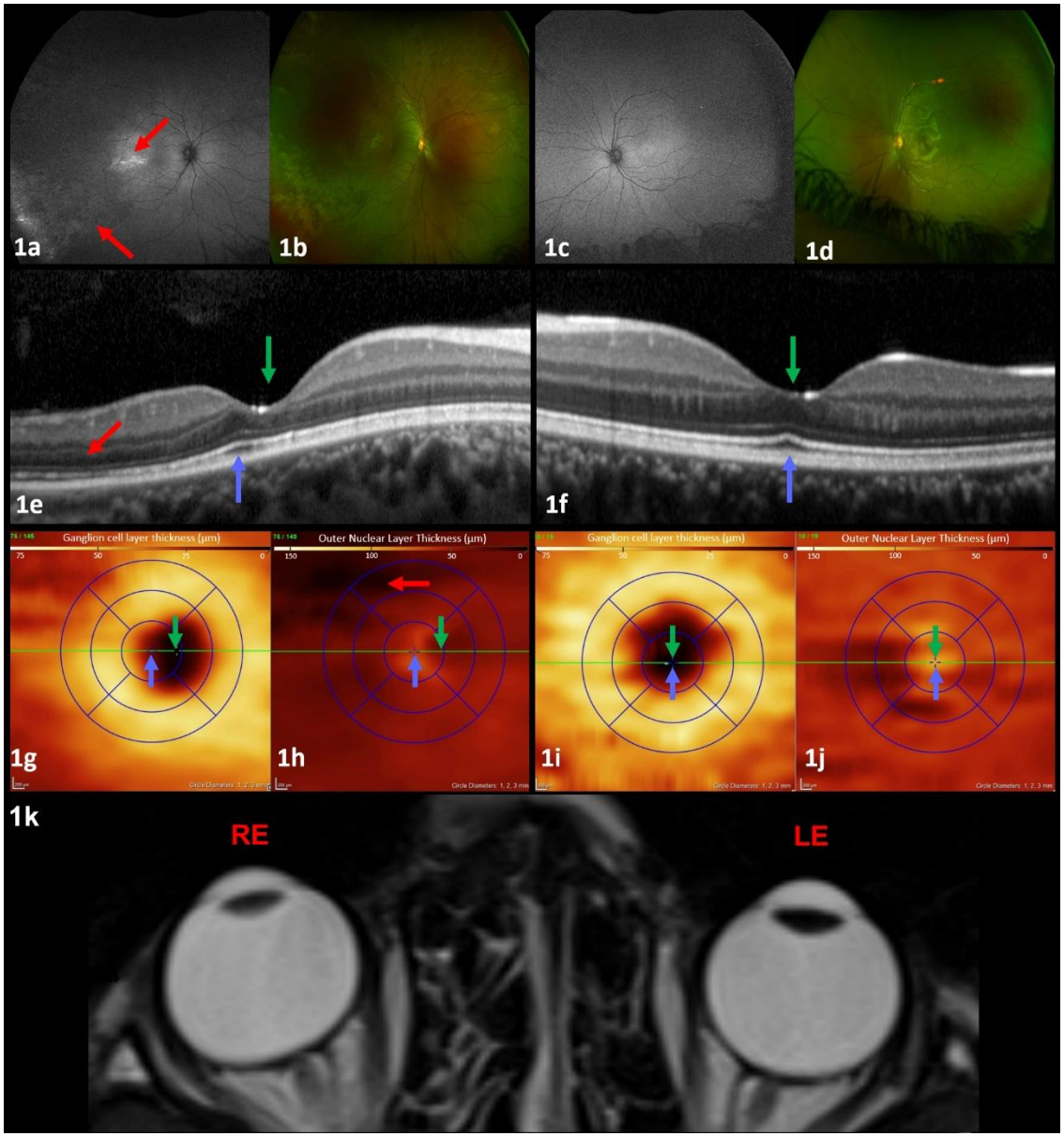
1a
1b
1c
1d
1e
1f
Ganglion cell layer thickness (µm)
Outer Nuclear Layer Thickness (µm)
1g
1h
1i
1j
1k
RE
LE

Figure 1 – Ophthalmic imaging findings in this patient.
Panels a-d are ultra-wide field retinal images. Figure 1a demonstrates a horizontal line of hyper FAF in the right macula with some peripheral extension into the inferior temporal retina (red arrows). Figure 1b highlights generalised peripheral mottled pigmentary change in the RE with an abnormal appearance in the inferior temporal retina. Figure 1c and 1d show the normal appearance of the fundus FAF and red-green wide-field colour images in the fellow LE. Figure 1e is an OCT axial section of RE retina whereby the morphology of the outer nuclear peak (blue arrow) is seen to be misaligned against the nasally placed foveal pit (green arrow). There is some disruption in the ellipsoid layer over the temporal macula (red arrow), which is corroborated by temporal thinning of the OPL in Figure 1h. Figure 1f from the LE shows normally formed foveal architecture, with outer nuclear layer thickness (ONTL) proportionately aligned with the foveal dip. Figure 1g demonstrates the tomographic ganglion cell layer thickness (GCLT) corresponding to the foveal pit in the RE, which appears to be nasally distorted (green arrow). Figure 1h shows the peak ONLT (blue arrow), which is displaced temporally relative to the foveal dip (green arrow). In Figure 1h there is ONLT thinning over the superior temporal retina (red arrow) corresponding to the outer segment atrophy. Figure 1i and 1j show GCLT and ONLT peak and troughs that are aligned typically (green and blue arrows). Figure 1k illustrates the MRI findings in this patient, showing subtle nasal globe flattening/temporal globe protrusion of the RE with respect to the LE.

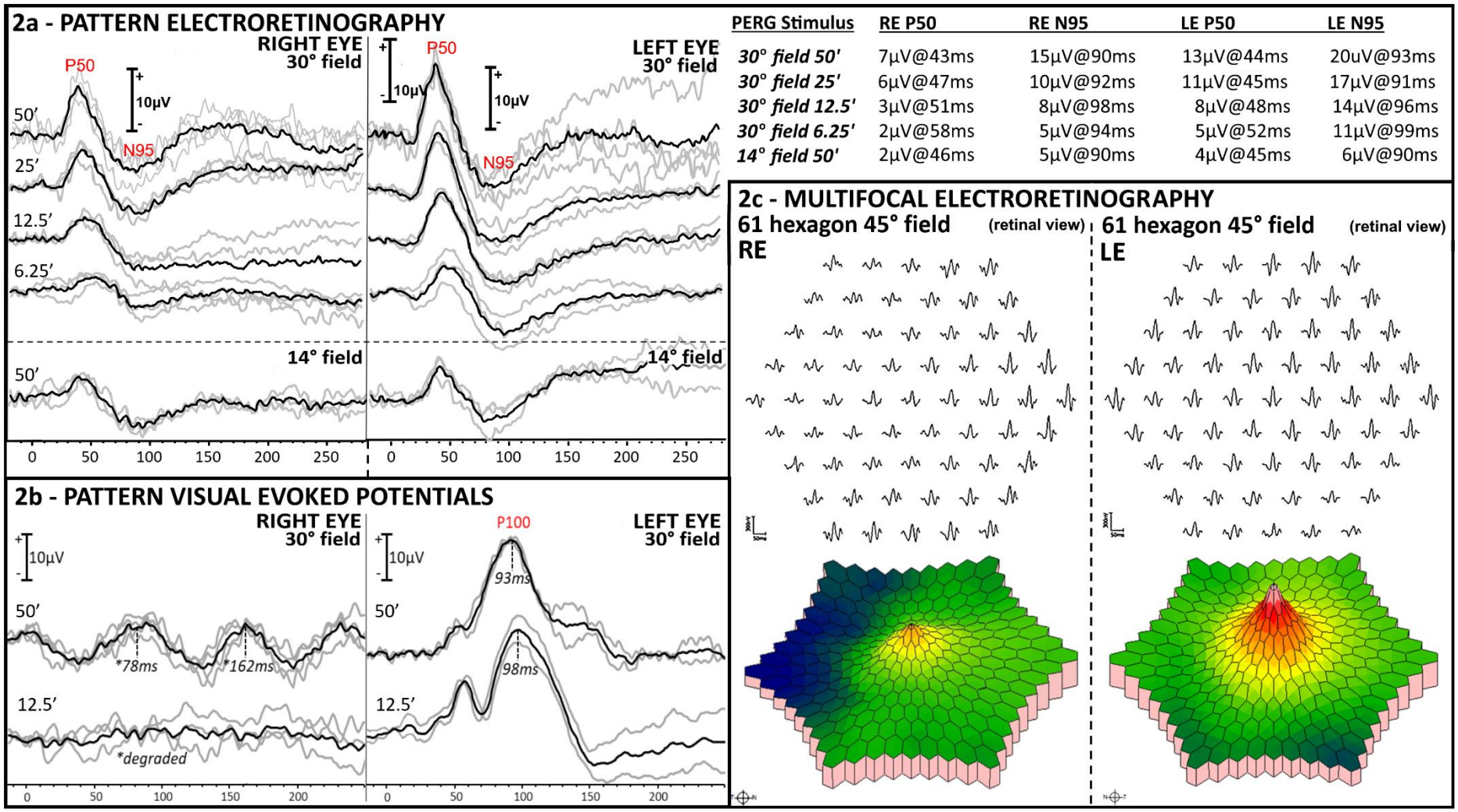

PERG Stimulus	RE P50	RE N95	LE P50	LE N95
30° field 50'	7μV@43ms	15μV@90ms	13μV@44ms	20uV@93ms
30° field 25'	6μV@47ms	10μV@92ms	11μV@45ms	17μV@91ms
30° field 12.5'	3μV@51ms	8μV@98ms	8μV@48ms	14μV@96ms
30° field 6.25'	2μV@58ms	5μV@94ms	5μV@52ms	11μV@99ms
14° field 50'	2μV@46ms	5μV@90ms	4μV@45ms	6μV@90ms

Figure 2 – PERG, PVEP& mfERG findings in the patient

These figures show the PERG (2a), PVEP (2b) and mfERG (2c) findings in our patient. From the top, PERGs to smaller check widths are presented in descending order for spatial frequency (minutes of arc) presented to each eye in a large 30° field, followed by the PERG produced to 50’ checks presented in

a standard 15° field size. PERGs from the LE were all within laboratory reference ranges with well defined P50 and N95 components and N95:P50 amplitude ratio. PERGs from the RE show is relative P50 amplitude reduction, which becomes more evident with mild prolongation in peak-time to smaller check widths (higher spatial frequencies), with preservation of the N95:P50 ratio. PERGs from a smaller 14 degree field also show an inter-ocular difference with smaller P50 from the RE relative to the LE. Quantified PERG data are shown in the top right of the image. Panel 2b shows the ISCEV standard PVEP waveforms from each eye to standard and small check widths, from the right eye atypically degraded and bifid, and unrecordable to small check wdiths, with those from the unaffected left eye within normal limits. Panel 2c show the mfERG trace arrays in retinal view and topographic maps from each eye to a 61 hexagon stimulus subtending a 45° field. The LE shows a well defined foveal peak. The RE foveal peak is smaller with a sector response suppression over the temporal/superior-temporal retina consistent with imaging findings. Colour plots are shown below for visualisation of the comparative topography of these waveforms from each eye.